

A complete next-to-leading order QCD description of resonant Z' production and decay into $t\bar{t}$ final states

Fabrizio Caola,^{1,*} Kirill Melnikov,^{1,†} and Markus Schulze^{2,‡}

¹*Department of Physics and Astronomy, Johns Hopkins University, Baltimore, USA*

²*Argonne National Laboratory (ANL), Lemont, IL 60439, USA*

We discuss QCD radiative corrections to the production of a heavy neutral resonance Z' at the LHC assuming that it decays into a $t\bar{t}$ final state. Compared to previous studies, our computation includes top quark decays as well as interference between the Z' signal process and the QCD $t\bar{t}$ background. The interference contribution appears for the first time at next-to-leading order (NLO) QCD and requires new one-loop amplitudes that are not present when signal and background are treated separately. We describe some examples of how QCD radiative corrections may influence both the exclusion limits and studies of properties of the new resonance, once it is discovered.

I. INTRODUCTION

Searches for physics beyond the Standard Model (BSM) at the LHC are starting to reach into the TeV mass range and exclude large fractions of parameter spaces of most popular models of New Physics. Many of these exclusion limits – that often involve rather complicated final states and extreme energies – are based on leading order calculations which are not necessarily adequate in such situations. While, in general, it is unrealistic to expect that theoretical description of collider processes that are relevant for all interesting BSM scenarios will be advanced to NLO QCD accuracy, this can be done for such extensions of the SM that are considered to be sufficiently robust. In fact, such calculations have been reported recently for a variety of New Physics models in Refs. [1–5].

One such robust scenario is an extension of the Standard Model by an additional $U(1)$ gauge group which generically leads to the appearance of a massive neutral flavor-conserving spin-one particle which we will refer to as Z' . Physics of such particle is reviewed in Refs. [6–8]; for recent discussions in the context of the LHC see e.g. Refs. [9–11]. Such a particle will, generically, couple to all quarks, including the top quark. For this reason, it can be searched for in the process $pp \rightarrow Z' \rightarrow t\bar{t}$ at the LHC. In fact, searches for Z' resonances in this process are well under way [12–17]. Currently, such searches exclude Z' with masses smaller than $1.5 \sim 2$ TeV where the exact value of the exclusion bound depends on the assumed couplings of the Z' to light quarks and the top quark.

In this paper we study the QCD corrections to the production of a Z' resonance with its subsequent decay to a $t\bar{t}$ pair without the simplifying assumptions of previous

studies. In particular, we include NLO QCD corrections to decays of top quarks into observable final states, account for all spin correlations and consider an interference of the signal $q\bar{q} \rightarrow Z' \rightarrow t\bar{t}$ with the background $q\bar{q} \rightarrow g^* \rightarrow t\bar{t}$ which appears at next-to-leading order for the first time.

Our computation can be used to perform realistic studies of both the discovery potential of $Z' \rightarrow t\bar{t}$ at the LHC as well as precision studies of the properties of the Z' resonance once it is discovered. These potential applications of our calculation are illustrated by computing K -factors for experimental cuts that are similar to the ones employed by ATLAS and CMS [12–17] in their searches for $Z' \rightarrow t\bar{t}$ and by studying kinematic distribution of a suitably-defined relative azimuthal angle of leptons from semileptonic decays of top quarks [18] that can be used to discriminate between vector and axial couplings of Z' to top quarks.

The rest of the paper is organized as follows. In Section II we describe the Z' model that we use throughout the paper and comment on the general set-up of the computation. In Section III we discuss aspects of the NLO QCD calculation that are relevant for our analysis. In Section IV we present the numerical results. We conclude in Section V.

II. SET-UP

In this Section we describe the set-up of the calculation. We present our results in the context of the leptophobic top-color model of Refs. [9, 19] which is the reference model used by the LHC experiments to present their exclusion limits. Note, however, that our calculation is more general since couplings of Z' to all quarks, the Z' mass and the Z' width are free parameters in the calculation.

In the context of the leptophobic top-color model, some of these parameters are correlated. Indeed, the Z' cou-

*Electronic address: caola@pha.jhu.edu

†Electronic address: melnikov@pha.jhu.edu

‡Electronic address: markus.schulze@anl.gov

	Narrow Z' , $\Gamma_{Z'}^{(\text{LO})} = 15 \text{ GeV}$				Broad Z' , $\Gamma_{Z'}^{(\text{LO})} = 150 \text{ GeV}$			
(f_1, f_2)	(1,1)	(-1,-1)	(1,0)	(0,-1)	(1,1)	(-1,-1)	(1,0)	(0,-1)
LO, $\mu = m_{Z'}/2$	3.94	3.76	5.73	2.13	39.0	36.4	56.6	20.9
LO, $\mu = m_{Z'}$	3.70	3.53	5.39	2.00	36.8	34.3	53.4	19.6
LO, $\mu = 2m_{Z'}$	3.49	3.32	5.08	1.88	34.7	32.4	50.5	18.5
NLO, $\mu = m_{Z'}/2$	4.20	3.90	6.11	2.21	42.0	38.2	61.0	21.9
NLO, $\mu = m_{Z'}$	4.17	3.89	6.06	2.20	41.7	38.1	60.5	21.8
NLO, $\mu = 2m_{Z'}$	4.12	3.86	5.98	2.18	41.3	37.8	59.9	21.7
K -factor, $\mu = m_{Z'}/2$	1.07	1.04	1.07	1.04	1.08	1.05	1.08	1.05
K -factor, $\mu = m_{Z'}$	1.13	1.10	1.12	1.10	1.13	1.11	1.13	1.11
K -factor, $\mu = 2m_{Z'}$	1.18	1.16	1.17	1.16	1.19	1.17	1.18	1.17

TABLE I: Cross-sections (in fb) for $pp \rightarrow Z' \rightarrow t\bar{t} \rightarrow \ell\bar{\ell}\nu\bar{\nu}jj + X$ at leading and next-to-leading order in perturbative QCD for various Z' models at the 14 TeV LHC. Results are shown for different choices of the renormalization and factorization scales. We use MSTW2008 parton distribution functions [23]. Kinematic cuts on leptons, jets and missing energy are specified in Section IV. The first column corresponds to purely vector Z' , the second one to purely axial Z' , the third one is the reference point used in experimental analysis by the ATLAS and CMS collaborations [12, 17].

pling to SM particles is described by the Lagrangian

$$\mathcal{L} = \frac{1}{2}g_1 \cot\theta_H Z'^{\mu} (J_{\mu}^L + J_{\mu}^R), \quad (1)$$

where g_1 is the weak coupling constant and $\cot\theta_H$ is the mixing parameter that encodes the overall deviation of the Z' couplings to quarks from the electroweak ones. The left- and right-handed currents are defined as $J_L^{\mu} = \bar{t}_L\gamma_{\mu}t_L + \bar{b}_L\gamma_{\mu}b_L - \bar{u}_L\gamma_{\mu}u_L - \bar{d}_L\gamma_{\mu}d_L$, and $J_R^{\mu} = f_1(\bar{t}_R\gamma_{\mu}t_R - \bar{u}_R\gamma_{\mu}u_R) + f_2(\bar{b}_R\gamma_{\mu}b_R - \bar{d}_R\gamma_{\mu}d_R)$. In the top-color model, one would require $f_1 \geq 0$ and/or $f_2 \leq 0$ in the right-handed current for top-color tilting [19].

Exclusion limits are often presented assuming $f_1 = 1$ and $f_2 = 0$ which corresponds to the vector coupling of Z' to top quarks but, of course, other choices of these parameters lead to richer physics. For this reason, we consider four different coupling choices in what follows, $(f_1, f_2) = (1, 1), (-1, -1), (1, 0), (0, -1)$. The first and the second cases correspond to pure vector or pure axial Z' couplings; the remaining choices describe mixed cases.

We can use the interaction Lagrangian Eq. (1) to compute the total decay width of the Z' -boson. At leading order we obtain

$$\Gamma_{Z'}^{\text{LO}} = \frac{\alpha \cot^2\theta_H m_{Z'}}{8 \cos^2\theta_W} \left[(3 + f_1^2 + 2f_2^2) + \beta_t \left((1 + f_1^2) - (1 - f_1^2 - 6f_1) \frac{m_t^2}{m_{Z'}^2} \right) \right], \quad (2)$$

where $\beta_t = \sqrt{1 - 4m_t^2/m_{Z'}^2}$. We therefore take $f_1, f_2, \Gamma_{Z'}^{\text{LO}}$ and the mass of the Z' resonance as free parameters of the theory and derive the overall coupling strength of Z' to quarks from them. We note that this leads to a strong correlation between the strength of couplings to quarks and the width of the resonance which may be less pronounced in other models. We will return to this issue later in the paper when discussing the importance of

the interference between signal and background processes that occurs at NLO QCD.

As we pointed out already, one of the goals of this paper is to present a realistic description of the hadronic $Z' \rightarrow t\bar{t}$ production process that combines QCD radiative corrections and top quark decays. To this end, we have implemented all the relevant top quark decay channels. For simplicity, we will only discuss results for fully leptonic channels in what follows. We use the narrow width approximation for top quark pair production as described in Ref. [20]. The parametric accuracy of this approximation is $\mathcal{O}(\Gamma_t/m_t)$ and its practical reliability is superb as long as the on-shell intermediate $t\bar{t}$ state is kinematically allowed [21].

For a complete NLO QCD analysis of the $pp \rightarrow Z' \rightarrow t\bar{t} \rightarrow XX$ process in the narrow width approximation for t and \bar{t} , we need the following ingredients:

- NLO QCD corrections to $pp \rightarrow Z' \rightarrow t\bar{t}$ for polarized t and \bar{t} .
- NLO QCD corrections to Z' decay width. Those corrections are potentially important to properly describe shapes of the $t\bar{t}$ invariant mass distribution when $\mathcal{O}(\alpha_s)$ corrections are taken into account. These corrections can be taken from the computation of $\mathcal{O}(\alpha_s)$ corrections to $Z \rightarrow b\bar{b}$ decay for massive b -quarks reported in Ref. [22].
- NLO QCD corrections to top quark decays, including NLO QCD corrections to the top quark width and the W width. All these corrections were already implemented in the calculation of $pp \rightarrow t\bar{t}$ reported in Ref. [20] and we take them from there.
- NLO QCD corrections to the QCD background process $pp \rightarrow t\bar{t}$. We use the implementation described in Ref. [20].

	Narrow Z' , $\Gamma_{Z'}^{(\text{LO})} = 15 \text{ GeV}$				Broad Z' , $\Gamma_{Z'}^{(\text{LO})} = 150 \text{ GeV}$			
(f_1, f_2)	(1,1)	(-1,-1)	(1,0)	(0,-1)	(1,1)	(-1,-1)	(1,0)	(0,-1)
LO	3.70	3.53	5.39	2.00	36.8	34.3	53.4	19.6
NLO production, $q\bar{q}$	4.93	4.74	7.17	2.67	49.4	46.3	71.6	26.4
NLO production, qg	-0.15	-0.14	-0.22	-0.08	-1.4	-1.2	-2.1	-0.7
NLO production, $g\bar{q}$	-0.02	-0.02	-0.03	-0.01	-0.2	-0.2	-0.3	-0.1
NLO decay	-0.60	-0.57	-0.87	-0.31	-6.1	-5.6	-8.8	-3.2
Interference with QCD	~ 0	-0.13	0.01	-0.06	~ 0	-1.3	0.1	-0.6
Full NLO	4.17	3.89	6.06	2.20	41.7	38.1	60.5	21.8
K -factor	1.13	1.10	1.12	1.10	1.13	1.11	1.13	1.11

TABLE II: Cross-sections (in fb) for $pp \rightarrow Z' \rightarrow t\bar{t} \rightarrow \ell\bar{\ell}\nu\bar{\nu}jj + X$ at the 14 TeV LHC split into different contributions, for the reference scale $\mu = m_{Z'} = 1.5 \text{ TeV}$. We use MSTW2008 parton distribution functions. Kinematic cuts on leptons, jets and missing energy are specified in Section IV. The leading order process, computed with NLO parameters (two-loop α_s , NLO PDFs and widths) is included in “NLO production, $q\bar{q}$ ” category.

- Interference of the background $q\bar{q} \rightarrow t\bar{t}$ and signal $q\bar{q} \rightarrow Z \rightarrow t\bar{t}$ processes that appears at NLO QCD for the first time.

To be specific, consider the pure QCD scattering amplitude for $q\bar{q} \rightarrow t\bar{t}$ through one-loop. Its color decomposition reads [20]

$$\mathcal{A}_{\text{QCD}} = g_s^2 \left(\delta_{i_q i_{\bar{t}}} \delta_{i_{\bar{t}} i_{\bar{q}}} - \frac{1}{N_c} \delta_{i_q i_{\bar{q}}} \delta_{i_{\bar{t}} i_{\bar{t}}} \right) A_{\text{QCD}}^{(0)} + g_s^4 \left[\delta_{i_q i_{\bar{t}}} \delta_{i_{\bar{t}} i_{\bar{q}}} \mathcal{B}_1 - \frac{1}{N_c} \delta_{i_q i_{\bar{q}}} \delta_{i_{\bar{t}} i_{\bar{t}}} \mathcal{B}_2 \right], \quad (4)$$

III. NLO QCD CORRECTIONS TO $pp \rightarrow Z' \rightarrow t\bar{t}$

In this Section, we describe some details pertinent to the computation of NLO QCD corrections to $pp \rightarrow Z' \rightarrow t\bar{t}$. Through $\mathcal{O}(\alpha_s)$, we can express the $q\bar{q} \rightarrow Z' \rightarrow t\bar{t}$ amplitude as

$$\mathcal{A}_{Z'} = \delta_{i_q i_{\bar{q}}} \delta_{i_{\bar{t}} i_{\bar{t}}} A_{Z'}^{(0)} + g_s^2 \left[\frac{N_c^2 - 1}{2N_c} \delta_{i_q i_{\bar{q}}} \delta_{i_{\bar{t}} i_{\bar{t}}} \mathcal{C}_1 + \left(\delta_{i_q i_{\bar{t}}} \delta_{i_{\bar{t}} i_{\bar{q}}} - \frac{1}{N_c} \delta_{i_q i_{\bar{q}}} \delta_{i_{\bar{t}} i_{\bar{t}}} \right) \mathcal{C}_2 \right], \quad (3)$$

where $N_c = 3$ is the number of colors. The one-loop contribution to the amplitude $\mathcal{A}_{Z'}$ is given by the two color-stripped primitive amplitudes \mathcal{C}_1 and \mathcal{C}_2 . \mathcal{C}_1 describes the amplitude with the same color flow as the tree-level one $A_{Z'}^{(0)}$; it is computed from vertex corrections to the production and decay stage of the process $q\bar{q} \rightarrow Z' \rightarrow t\bar{t}$. It also receives contributions from the required renormalization constants. The function \mathcal{C}_2 receives contributions from box diagrams where a gluon and a Z' connect the initial $q\bar{q}$ and the final $t\bar{t}$ states.

It is clear from Eq.(3) that the amplitude \mathcal{C}_2 corresponds to the color-octet flow in the s -channel while the amplitude \mathcal{C}_1 and the tree-level amplitude $A_{Z'}^{(0)}$ correspond to the color-singlet flow in the s -channel. For this reason, \mathcal{C}_2 does not contribute to the production cross-section of Z' if we restrict ourselves to the underlying process $q\bar{q} \rightarrow Z' \rightarrow t\bar{t}$. On the other hand, we note that the color octet amplitude can interfere with the background process $q\bar{q} \rightarrow g^* \rightarrow t\bar{t}$. Such interference is not expected to be large for the narrow resonance but it is not clear a priori if it is negligible for broader resonances.

where tree- and one-loop contributions are separated. It follows from Eqs. (3,4) that the tree-level QCD amplitude $A_{\text{QCD}}^{(0)}$ can interfere with \mathcal{C}_2 . We can also see from Eq. (4) that, at one loop, \mathcal{A}_{QCD} contains the amplitude \mathcal{B}_2 whose color flow is equivalent to the color-singlet exchange in the s -channel. For this reason, \mathcal{B}_2 interferes with the tree-level amplitude for the Z' -production $A_{Z'}^{(0)}$, but \mathcal{B}_2 does not contribute to pure QCD process $q\bar{q} \rightarrow t\bar{t}$ due to the color structure of the $q\bar{q} \rightarrow g^* \rightarrow t\bar{t}$ amplitude at leading order. Therefore if we consider the physical process $q\bar{q} \rightarrow t\bar{t}$ that can be mediated by both gluon and Z' exchanges and if we allow for the interference effects between the two processes – that a priori are not obviously negligible for broad Z' resonances – two amplitudes beyond what has been so far considered in the literature are required. We compute those amplitudes and include the effects of the interference between signal and background processes in the discussion below.

We note that we neglect contributions of the one-loop “anomaly-like” diagrams $gg \rightarrow Z' \rightarrow t\bar{t}$ that are mediated by quark loops. Such contributions are expected to be negligible for several reasons. First, the gluon flux at center of mass energies relevant for Z' production is expected to be about one tenth of the $q\bar{q}$ flux. Second, the anomaly-free nature of the effective Lagrangian Eq. (1) ensures that $gg \rightarrow Z'$ vanishes identically if all quarks are massless. The quality of the massless approximation for top quarks in $gg \rightarrow Z'$ amplitude is controlled by the ratio of the top quark mass to the Z' mass which is quite small for values of the Z' mass that are of interest to us. We conclude that the double suppression caused by the

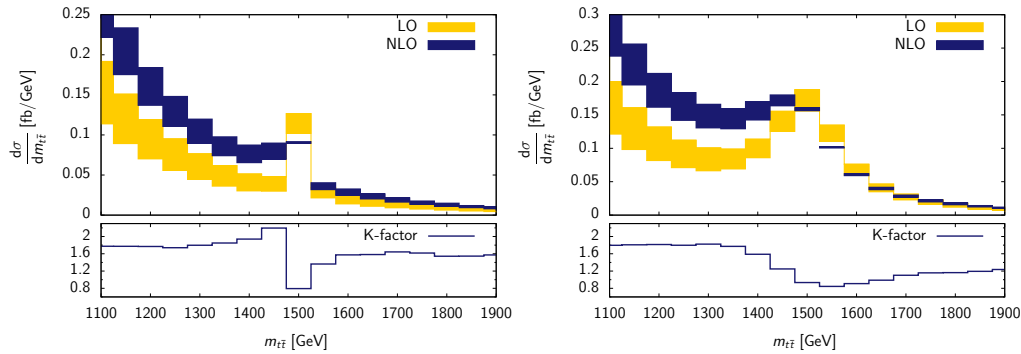


FIG. 1: Top-antitop invariant mass distribution in the reaction $pp \rightarrow t\bar{t}$ for $m'_{Z'} = 1.5$ TeV at the 14 TeV LHC at leading and next-to-leading order in perturbative QCD. Left pane: narrow Z' , $\Gamma'_{Z'} = 15$ GeV and $f_1 = 1, f_2 = 0$. Right pane: broad Z' , $\Gamma'_{Z'} = 150$ GeV and $f_1 = -1, f_2 = -1$. We use MSTW2008 parton distribution functions. Kinematic cuts on leptons, jets and missing energy are specified in Section IV. The K -factors are computed for the central scale choice $\mu = m_{Z'}$.

smallness of the gluon flux and the validity of the massless approximation for top quarks allows us to neglect the “anomaly” contribution.

The second point that we would like to emphasize are the QCD corrections to the Z' width. In general, we write the Z' propagator in the unitary gauge as

$$\mathcal{D}_{\mu\nu}^{Z'} = \frac{i}{k^2 - m_{Z'}^2 + im_{Z'}\Gamma_{Z'}} \left(-g_{\mu\nu} + \frac{k_\mu k_\nu}{m_{Z'}^2} \right). \quad (5)$$

The longitudinal part of the Z' propagator is not important since it always couples to the massless quark line on the “production side” of the process. When NLO QCD corrections to the production of Z' are considered, it is essential to include corrections to $\Gamma'_{Z'}$ in the denominator of the Z' propagator of Eq. (5). To see this, consider production of a narrow Z' , such that $\sigma(pp \rightarrow Z' \rightarrow t\bar{t}) \approx \sigma(pp \rightarrow Z') \times \text{Br}(Z' \rightarrow t\bar{t})$. To correctly compute the change in the branching ratio of $Z' \rightarrow t\bar{t}$ at NLO QCD, we need to account for corrections to the partial width $Z' \rightarrow t\bar{t}$ that we do by computing QCD corrections as described above *and* for the corrections to the total width $\Gamma_{Z'}$ that we have to compute separately and include into a Breit-Wigner propagator. We read off the NLO QCD corrections to the Z' width from the calculation of QCD corrections to the decay rate $Z \rightarrow b\bar{b}$ described in Ref. [22] where they are given as functions of $m_b/m_{Z'}$. For numerical examples that we consider below $m_t/m_{Z'} \ll 1$ and in that limit corrections to the width become simple. Indeed, if we use the massless top quark limit, the NLO width is just $(1 + \alpha_s/\pi)$ times the LO width. Nevertheless, in our calculation, we retain full $m_t/m_{Z'}$ dependence of the width following Ref. [22].

IV. NUMERICAL RESULTS

In this Section we illustrate our computation by presenting some numerical results. We consider the LHC with $\sqrt{s} = 14$ TeV center-of-mass energy. We consider

semi-leptonic decays of both t and \bar{t} . We use the anti- k_t jet algorithm with $R = 0.5$ and impose cuts on the final state particles that are motivated by current Z' searches [12, 17]. In particular, we require $p_{\perp, \text{lep}} < 20$ GeV, $|\eta_{\text{lep}}| < 2.5$, $p_{\perp, \text{jet}} < 30$ GeV, $|\eta_{\text{jet}}| < 2.5$. We choose $m_{Z'} = 1.5$ TeV, which is close to the current exclusion limits for our choices of the Z' couplings. We use the MSTW2008 parton distribution functions [23].

As pointed out in the Introduction, instead of specifying the mixing angle θ_H we find it more convenient to use the leading order width as an input parameter. We choose two reference values $\Gamma_{Z'}^{\text{LO}} = 15$ GeV (narrow Z') and $\Gamma_{Z'}^{\text{LO}} = 150$ GeV (broad Z'). We also choose $m_{Z'}$ as a reference value for the renormalization and factorization scales and show results for three choices $\mu = m_{Z'}/2, m_{Z'}$ and $2m_{Z'}$. We note that, most likely, this procedure overestimates the theoretical uncertainty since it implies a scan over a very broad range of scales, between $\mu = 750$ GeV and 3 TeV.

We summarize our results for production cross-sections in the di-lepton channel for both narrow and broad Z' resonance in Table I. The inclusion of NLO QCD corrections leads to extremely stable results under changes of the renormalization/factorization scales. The residual scale dependence is of the order of one percent. The mild scale dependence is in part due to the fact that the LO result does not explicitly depend on α_s so that the scale variation only comes from parton distribution functions. For $\mu = m_{Z'}$, we find that the NLO QCD corrections enhance the production cross-section by about ten percent, so that the corresponding K -factor is 1.1. This value is somewhat lower than $K \approx 1.3$ reported in Ref. [2] and we attribute this difference to our use of MSTW2008 parton distribution functions, kinematic cuts on top quark decay products and inclusion of radiative corrections to top quark decays. We note that we can reproduce the results for the NLO QCD K -factors reported in Ref. [2] if we use the set up for the calculation described in that reference.

To understand the importance of various NLO QCD ef-

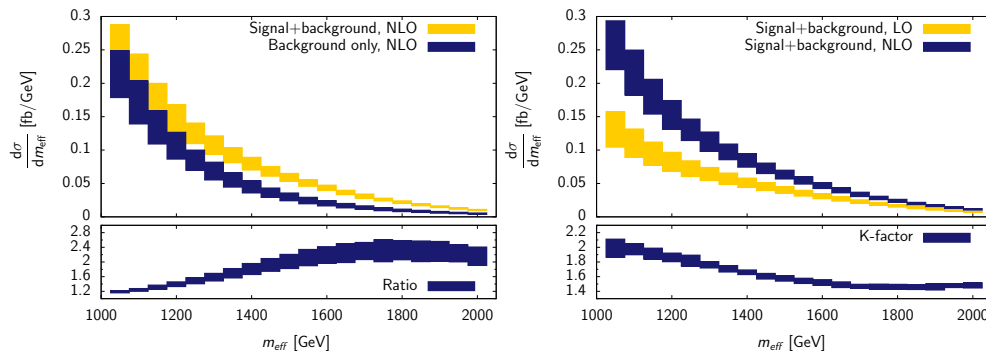


FIG. 2: Distribution of the effective mass defined as the sum of the transverse missing energy and H_{\perp} for broad $f_1 = f_2 = -1$ Z' at the 14 TeV LHC. We use MSTW2008 parton distribution functions. Kinematic cuts on leptons, jets and missing energy are specified in Section IV.

fects, we display in Table II all the different contributions to the NLO cross section for $\mu = m_{Z'}$. The “production” contribution corresponds to NLO QCD corrections to various production processes $pp \rightarrow Z' \rightarrow t\bar{t}$ and leading order top quark decays. We include the leading order process $q\bar{q} \rightarrow Z' \rightarrow t\bar{t}$ computed with the QCD-corrected values of $\Gamma_{Z'}$ and Γ_t in the “production” contribution. The “decay” contribution corresponds to leading order $q\bar{q} \rightarrow Z' \rightarrow t\bar{t}$ and NLO QCD decay of t and \bar{t} . The negative correction from the decay somewhat compensates the positive change in the leading order processes caused by using Γ_t^{NLO} there, but the cancellation is not complete because of the fiducial volume cuts. Finally, the last contribution displayed in Table II refers to the interference between QCD amplitudes and Z' amplitudes that arises at NLO QCD as we already discussed.

An interesting feature of these results is that although the $q\bar{q}$ channel gives the largest contribution and it has an associated K -factor of about 1.3 similar to the result adopted in a recent analysis by ATLAS and CMS collaborations [12, 17], all other contributions to the K -factor are negative.¹ The net effect of these corrections is the reduction of the K -factor to a smaller value $K \sim 1.1$.

We also note that the relevance of the interference between signal and background production processes depends on the details of the model. For the Z' model that we employ in this paper, the interference can reach a few percent but it can be larger in general. The interference is absent for pure vector couplings of Z' due to Furry’s theorem and it is maximal for pure axial couplings. For the model specified by the Lagrangian Eq. (1) the magnitude of interference contributions can be as large as the production contribution in the $q\bar{q}$ channel.

The interference effects become more relevant for broader Z' resonances. While this is expected feature of the result, it is perhaps not as apparent in Table II as it should be, so we comment on how to properly interpret what is seen there. Indeed, a glance at Table II suggests that the relative importance of the interference is similar for narrow and broad Z' . However, this is an artifact of our model choice where the growth of the Z' width is correlated with the growth of the Z' couplings to quarks. Since the production cross-sections for $pp \rightarrow Z' \rightarrow t\bar{t}$ is *quadratic* in those couplings, while the interference is *linear*, the fact that both the cross-section and the interference increase by an order of magnitude for the broad Z' compared to narrow Z' suggests that the relative importance of the interference increased by a factor of three. Hence, we conclude that such interference effects can be important for broad resonances especially if the width of the resonance is only weakly correlated with its coupling to quarks. We note that this interference contribution can play a role in such observables as the top quark forward-backward asymmetry at the Tevatron. Although a flavor-conserving Z' resonance in the s -channel is already ruled out as a possible explanation for the observed asymmetry, it is interesting to note that the NLO QCD interference contribution to the asymmetry in our reference model can be as large as 20% of the leading order asymmetry generated by Z' exchange. The size of the effect suggests that it is worthwhile to study it for more realistic models that explain the Tevatron asymmetry. We leave this for future work.

We now proceed to the discussion of selected differential distributions. We begin with the distribution in the $t\bar{t}$ invariant mass. While the $t\bar{t}$ invariant mass is difficult to reconstruct in the di-lepton channel, it is still instructive to look at the generic features of this distribution. Such distributions for narrow and broad Z' are shown in Fig. 1 where we also include the contribution from $pp \rightarrow t\bar{t}$ background process at leading and next-to-leading order in perturbative QCD. We employ the reference parameter choice $(f_1, f_2) = (1, 0)$ and $(f_1, f_2) = (-1, -1)$ respectively for the narrow and broad

¹ We mention that ATLAS and CMS use these K -factors for 7 and 8 TeV LHC, whereas we have only shown results for 14 TeV LHC. We have, however, calculated the K -factor for 7 TeV LHC for the narrow Z' with the mass of 1.5 TeV for the coupling choice $f_1 = 1, f_2 = 0$ and fiducial cuts as described in the text and found $K = 1.1$ for $\mu = m_{Z'}$.

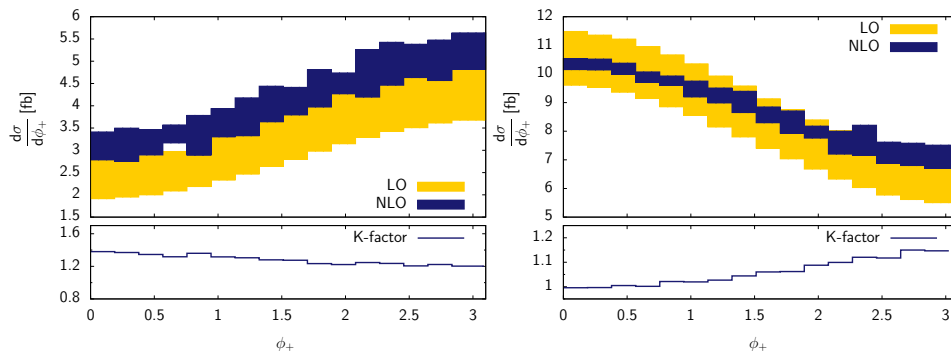


FIG. 3: Distributions of ϕ_+ variable, introduced in [18], at leading and next-to-leading order in QCD at 14 TeV LHC. Both signal and background are included in the $|m_{t\bar{t}} - m_{Z'}| < 100$ GeV window. Left pane: narrow (1,0) Z' model. Right pane: broad (-1,-1) Z' . We use MSTW2008 parton distribution functions. Kinematic cuts on leptons, jets and missing energy are specified in Section IV.

Z' cases reported in Fig. 1. The $m_{t\bar{t}}$ invariant mass distribution shows expected features – the Z' peak which is very prominent at leading order becomes broader and less prominent at NLO QCD since a significant fraction of events is shifted to lower $m_{t\bar{t}}$ values because of the final state radiation. As the result, the K -factor changes significantly around the peak position, for both narrow and broad Z' . This rapid change in the K -factor may be invisible for the narrow Z' , given that the resolution of $m_{t\bar{t}}$ is close to a hundred GeV but it may become important for broader resonances. Indeed, as follows from the right pane of Fig. 1, the K -factor changes by almost a factor of two, from $K = 1.8$ at $m_{t\bar{t}} = 1300$ GeV to $K = 0.8$ at $m_{t\bar{t}} = 1600$ GeV despite the fact that the average K -factor is relatively modest. Note that the K -factor at lower invariant mass values – which are more accessible experimentally – is actually quite significant and it almost doubles the expected cross-section there. As a further illustration of this point, we note that the peak of the NLO QCD $m_{t\bar{t}}$ distribution for a broad Z' shown in the right pane of Fig. 1 is located in a different bin when compared to the leading order $m_{t\bar{t}}$ distribution.

Our calculation allows to compute any kinematic distribution that is relevant for Z' production through NLO QCD and, in particular, those that are defined using momenta of top quark decay products. For illustration purposes, we show two of such distributions. In Fig. 2 the distribution of the effective mass for events with and without (broad) Z' is shown. All NLO QCD effects that are described above are included in the calculation. Understanding the effective mass distribution is of paramount importance for the experimental analysis, where it is used to extract information about the Z' mass in channels where direct reconstruction of $m_{t\bar{t}}$ is not possible. It follows from the the right pane of Fig. 2 that the K -factor is a rapidly changing function of m_{eff} . This is the consequence of the fact that the m_{eff} distribution receives contributions from signal and background processes which have markedly different dependence on m_{eff} and very different K -factors.

As another example, we show a kinematic distribution that can be constructed if lepton momenta are accurately measured. As was pointed out in Ref. [18], such distributions are useful for exploring the Lorentz structure of the couplings of the new resonance to top quarks. Since our NLO QCD computation includes the spin correlations exactly, we can extend the discussion of the relevant kinematic distributions by including NLO QCD corrections.

We consider the kinematic distribution of the azimuthal angle ϕ_+ which is constructed in the following way [18]. We work in the center-of-mass frame² of t and \bar{t} . In that frame the directions of the incoming protons are not back to back; we denote them as n_1 and n_2 . We define a three-vector $\vec{n}_{12} = (\vec{n}_1 - \vec{n}_2)/|\vec{n}_1 - \vec{n}_2|$ and form a coordinate system by taking the z -axis to be the direction of the top momentum \vec{n}_t , the x -axis to be \vec{n}_{12} and the y -axis to be $\vec{n}_t \times \vec{n}_{12}$. We now write the momenta of the lepton and the anti-lepton in that reference frame as $p_{l,\bar{l}} = E_{l,\bar{l}} (1, \sin \vartheta \cos \varphi_{l,\bar{l}}, \sin \vartheta \sin \varphi_{l,\bar{l}}, \cos \theta_{l,\bar{l}})$ and define the angle ϕ_+ as $\phi_+ = \cos^{-1} (\cos \varphi_l \cos \varphi_{\bar{l}} - \sin \varphi_l \sin \varphi_{\bar{l}})$. As was pointed out in Ref. [18], the ϕ_+ distribution can be used to discriminate between vector and axial couplings of Z' to $t\bar{t}$ pair.

We show the results of the computation of the ϕ_+ distribution in Fig. 3 where two scenarios *i*) narrow Z' with $f_1 = 1$ and $f_2 = 0$ and *ii*) broad Z' with $f_1 = f_2 = -1$ are shown. The distributions contain t and \bar{t} from both the QCD background process and from the Z' production. To reduce contribution of the background, we require that the invariant mass of the $t\bar{t}$ system satisfies the constraint $|m_{t\bar{t}} - m_{Z'}| < 100$ GeV. With this cut, the signal-to-background ratio is roughly 0.5 for the narrow resonance and is close to a factor of two for the broad

² Because of the missing energy in dilepton events, it is difficult, but not impossible, to reconstruct the $t\bar{t}$ center-of-mass frame. See the discussion of this point in Ref. [18].

resonance case. It follows from Fig. 3 that the shape of this distribution is fairly stable against NLO QCD radiative corrections although in case *ii*) (right pane) the QCD corrections have an effect of making the distribution more flat. Since a small admixture of a vector coupling will have a similar effect on that distribution, it is essential to accommodate radiative corrections for the precise measurement of $Z't\bar{t}$ couplings.

V. CONCLUSION

In this paper, we discussed NLO QCD radiative corrections to the production of a Z' boson in the reaction $pp \rightarrow Z' \rightarrow t\bar{t}$. In contrast to previous studies, our computation includes interference effects of the Z' production process and the QCD background process that may become relevant for broad resonances. In addition, we include radiative corrections to top quark decays, keeping all spin correlations intact. We find that the NLO QCD corrections increase leading order cross-sections by a modest amount that is somewhat smaller than what has been adopted in recent studies by the ATLAS and CMS collaborations [12, 17]. We also find that radiative corrections to $t\bar{t}$ invariant mass distribution and to the effective mass distribution are significant and strongly-dependent on $m_{t\bar{t}}$ and m_{eff} , respectively. For broader resonances,

they increase the number of events with smaller invariant mass of the $t\bar{t}$ system making heavier resonances more accessible experimentally.

Our calculation is useful for understanding the Lorentz structure of Z' interaction with the $t\bar{t}$ pair with high accuracy once the resonance is discovered. We have illustrated this by computing the distribution in the relative angles of lepton and antilepton defined as suggested in Ref. [18]. This variable was found [18] to be a good discriminator between vector and axial couplings of Z' to top quarks; our computation allows to check if this conclusion remains valid when NLO QCD corrections are included. We found that, in case of the narrow Z' , the effect of QCD radiative corrections is to rescale this distribution by an overall factor without changing its shape while the situation with broader Z' is somewhat more complicated. At any rate, our calculation makes it possible to analyze any Z' scenario with NLO QCD accuracy. We look forward to the confrontation of our computation with LHC data.

Acknowledgments This research is partially supported by US NSF under grants PHY-1214000 and by US DOE under grants DE-AC02-06CD11357. Calculations reported in this paper were performed on the Homewood High Performance Cluster of the Johns Hopkins University.

-
- [1] Z. Sullivan, Phys. Rev. D **66**, 075011 (2002) [hep-ph/0207290].
 - [2] J. Gao, C. S. Li, B. H. Li, C. -P. Yuan and H. X. Zhu, Phys. Rev. D **82**, 014020 (2010) [arXiv:1004.0876 [hep-ph]].
 - [3] R. S. Chivukula, A. Farzinia, E. H. Simmons and R. Foadi, Phys. Rev. D **85**, 054005 (2012) [arXiv:1111.7261 [hep-ph]].
 - [4] D. Goncalves-Netto, D. Lopez-Val, K. Mawatari, T. Plehn and I. Wigmore, arXiv:1211.0286 [hep-ph].
 - [5] H. X. Zhu, C. S. Li, D. Y. Shao, J. Wang and C. P. Yuan, arXiv:1201.0672 [hep-ph].
 - [6] P. Langacker, Rev. Mod. Phys. **81**, 1199 (2009) [arXiv:0801.1345 [hep-ph]].
 - [7] A. Leike, Phys. Rept. **317**, 143 (1999) [hep-ph/9805494].
 - [8] J. L. Hewett and T. G. Rizzo, Phys. Rept. **183**, 193 (1989).
 - [9] R. M. Harris and S. Jain, Eur. Phys. J. C **72**, 2072 (2012) [arXiv:1112.4928 [hep-ph]].
 - [10] L. Basso, K. Mimasu and S. Moretti, JHEP **1211**, 060 (2012) [arXiv:1208.0019 [hep-ph]].
 - [11] J. de Blas, J. M. Lizana and M. Perez-Victoria, arXiv:1211.2229 [hep-ph].
 - [12] G. Aad *et al.* [ATLAS Collaboration], Eur. Phys. J. C **72**, 2083 (2012) [arXiv:1205.5371 [hep-ex]].
 - [13] G. Aad *et al.* [ATLAS Collaboration], JHEP **1209**, 041 (2012) [arXiv:1207.2409 [hep-ex]].
 - [14] G. Aad *et al.* [ATLAS Collaboration], arXiv:1211.2202 [hep-ex].
 - [15] S. Chatrchyan *et al.* [CMS Collaboration], JHEP **1209**, 029 (2012) [arXiv:1204.2488 [hep-ex]].
 - [16] S. Chatrchyan *et al.* [CMS Collaboration], arXiv:1209.4397 [hep-ex].
 - [17] S. Chatrchyan *et al.* [CMS Collaboration], arXiv:1211.3338 [hep-ex].
 - [18] M. Baumgart and B. Tweedie, JHEP **1109**, 049 (2011) [arXiv:1104.2043 [hep-ph]].
 - [19] R. M. Harris, C. T. Hill and S. J. Parke, hep-ph/9911288.
 - [20] K. Melnikov and M. Schulze, JHEP **0908**, 049 (2009) [arXiv:0907.3090 [hep-ph]].
 - [21] See contribution by A. Denner, S. Dittmaier, S. Kallweit, S. Pozzorini and M. Schulze in J. Alcaraz Maestre *et al.* [SM AND NLO MULTILEG and SM MC Working Groups Collaboration], arXiv:1203.6803 [hep-ph].
 - [22] B. A. Kniehl and J. H. Kuhn, Nucl. Phys. B **329**, 547 (1990).
 - [23] A. D. Martin, W. J. Stirling, R. S. Thorne and G. Watt, Eur. Phys. J. C **63**, 189 (2009) [arXiv:0901.0002 [hep-ph]].